

THE ANALYSIS OF THE BOUNDARY CONDITIONS FOR THE COMPRESSIBLE GAS FLOW AS A MODIFICATION OF THE RIEMANN PROBLEM

M. Kyncl, J. Pelant ¹

Abstract: *We work with the system of equations describing non-stationary compressible turbulent fluid flow (2D,3D), i.e. the Reynolds-Averaged Navier-Stokes (RANS) equations, and we focus on the numerical solution of these equations and on the boundary conditions. Some boundary conditions (i.e. fixed, linearized) bring non-physical errors into the solution, which may lead to the wrong results. We use the analysis of the Riemann problem for the construction of the boundary conditions in order to match the experimental data. Within this problem we show, that the unknown one-side initial condition can be partially replaced by the suitable complementary condition. We suggest such complementary conditions (by the preference of total quantities, pressure, temperature, velocity, condition at the diffusible barrier,...) in order to match the physically relevant data. Algorithms were coded and used within our own developed code (using the finite volume method) for the solution of the Euler, NS, and the RANS equations. Numerical examples show superior behavior of these boundary conditions.*

Keywords: *compressible gas flow, the Riemann problem, boundary conditions.*

1. Introduction

The physical theory of the compressible fluid motion is based on the principles of conservation laws of mass, momentum, and energy. The mathematical equations describing these fundamental conservation laws form a system of partial differential equations (the Euler Equations, the Navier-Stokes Equations, the Navier Stokes Equations with turbulent models). In this work we focus on the numerical solution of these equations. The correct design of the boundary conditions plays also an important role in the numerical modeling of the processes involved. We choose the well-known finite volume method to discretize the analytical problem, represented by the system of the equations in generalized (integral) form. To apply this method we split the area of the interest into the elements, and we construct a piecewise constant solution in time. The crucial problem of this method lies in the evaluation of the so-called fluxes through the edges/faces of the particular elements. In order to compute these fluxes, various methods can

¹ RNDr. Martin Kyncl, Ph.D., RNDr. Jaroslav Pelant, CSc., Výzkumný a zkušební letecký ústav, VZLÚ, Beranových 130, 199 05 Praha - Letňany, Czech Republic, tel. +420 225 115 521, e-mail kyncl@vzlu.cz, pelant@vzlu.cz

be used. One of the most accurate method (and perhaps the most accurate method) is based on the solution of the so-called Riemann problem for the 2D/3D split Euler equations. Unfortunately, the exact solution of this problem cannot be expressed in a closed form, and has to be computed by an iterative process (to given accuracy). Therefore this method is also one of the most demanding. In our work we decided to use the analysis of the exact solution also for the discretization of the fluxes through the boundary edges/faces. The right-hand side initial condition, forming the local Riemann problem, is not known at the boundary faces. In some cases (far field boundary) it is wise to choose the right-hand side initial condition here as the solution of the local Riemann problem with given far field values, which gives better results than the solution of the linearized Riemann problem, see Dolejsi (2006). Another boundary condition based on the exact Riemann problem solution, simulating the impermeable wall on move, was shown in (TORO, 1997, pages 221-225), where the right-hand side initial condition is constructed in a special way, in order to obtain the desired solution. We show, that the right-hand side initial condition for the local problem can be partially replaced by the suitable complementary condition. This idea was introduced by RNDr. Jaroslav Pelant, CSc. in PelantWork (1996-2000). In this work we analyze the modified local problems equipped with various complementary conditions. We construct own algorithms for the solution of the boundary problem, and we use it in the numerical examples.

2. The system of equations

We consider the conservation laws for viscous compressible turbulent flow with the zero outer volume forces and heat sources in a domain $\Omega \in \mathbb{R}^N$, and time interval $(0, T)$, with $T > 0$. The system of the Reynolds-Averaged Navier-Stokes equations in 3D has the form

$$\frac{\partial \mathbf{w}}{\partial t} + \sum_{s=1}^3 \frac{\partial \mathbf{f}_s(\mathbf{w})}{\partial x_s} = \sum_{s=1}^3 \frac{\partial \mathbb{R}_s(\mathbf{w}, \nabla \mathbf{w})}{\partial x_s} \quad \text{in } Q_T = \Omega \times (0, T). \quad (1)$$

Here x_1, x_2, x_3 are the space coordinates, t the time. $\mathbf{w} = \mathbf{w}(x, t) = (\varrho, \varrho v_1, \varrho v_2, \varrho v_3, E)^T$ is the state vector, $x \in \Omega$, t denotes the time, Q_T is called a space-time cylinder, $\mathbf{f}_s = (\varrho v_s, \varrho v_s v_1 + \delta_{s1} p, \varrho v_s v_2 + \delta_{s2} p, \varrho v_s v_3 + \delta_{s3} p, (E + p) v_s)^T$ are the inviscid fluxes, δ_{ij} is the Kronecker delta, $\mathbf{v} = (v_1, v_2, v_3)^T$ denotes the velocity vector, ϱ is the density, p the pressure, θ the absolute temperature, $E = \varrho e + \frac{1}{2} \varrho \mathbf{v}^2$ the total energy, $\mathbb{R}_s = (0, \tau_{s1}, \tau_{s2}, \tau_{s3}, \sum_{r=1}^3 \tau_{sr} v_r + C_k \partial \theta / \partial x_s)^T$ are the viscous fluxes, μ is the dynamic viscosity coefficient dependent on temperature, μ_T is the eddy-viscosity coefficient, and $\tau_{ij} = \begin{cases} (\mu + \mu_T) S_{ij}, & i \neq j \\ (\mu + \mu_T) S_{ij} - \frac{2}{3} \varrho k, & i = j \end{cases}$, where

$$\begin{aligned} S_{11} &= \frac{2}{3} \left(2 \frac{\partial v_1}{\partial x_1} - \frac{\partial v_2}{\partial x_2} - \frac{\partial v_3}{\partial x_3} \right), & S_{12} &= \frac{\partial v_1}{\partial x_2} + \frac{\partial v_2}{\partial x_1}, & S_{13} &= \frac{\partial v_1}{\partial x_3} + \frac{\partial v_3}{\partial x_1}, \\ S_{21} &= S_{12}, & S_{22} &= \frac{2}{3} \left(-\frac{\partial v_1}{\partial x_1} + 2 \frac{\partial v_2}{\partial x_2} - \frac{\partial v_3}{\partial x_3} \right), & S_{23} &= \frac{\partial v_2}{\partial x_3} + \frac{\partial v_3}{\partial x_2}, \\ S_{31} &= S_{13}, & S_{32} &= S_{23}, & S_{33} &= \frac{2}{3} \left(-\frac{\partial v_1}{\partial x_1} - \frac{\partial v_2}{\partial x_2} + 2 \frac{\partial v_3}{\partial x_3} \right). \end{aligned}$$

For the specific internal energy $e = c_v \theta$ we assume the caloric equation of state $e = p / \varrho (\gamma - 1)$, c_v is the specific heat at constant volume, $\gamma > 1$ is called the *Poisson adiabatic constant*. Further C_k is the heat conduction coefficient $C_k = \left(\frac{\mu}{P_r} + \frac{\mu_T}{P_{rT}} \right) c_v \gamma$, and P_r is laminar and P_{rT} is turbulent Prandtl constant number.

In this work we assume the system (1) equipped with the two-equation turbulent model $k - \omega$ (Kok), described in Kok (2000). The effective turbulent viscosity is $\mu_T = \varrho k / \omega$.

$$\begin{aligned} \frac{\partial \rho k}{\partial t} + \frac{\partial \rho k v_1}{\partial x_1} + \frac{\partial \rho k v_2}{\partial x_2} + \frac{\partial \rho k v_3}{\partial x_3} &= P_k - \beta^* \rho \omega k + \frac{\partial}{\partial x_1} \left((\mu + \sigma_k \mu_T) \frac{\partial k}{\partial x_1} \right) + \\ &+ \frac{\partial}{\partial x_2} \left((\mu + \sigma_k \mu_T) \frac{\partial k}{\partial x_2} \right) + \frac{\partial}{\partial x_3} \left((\mu + \sigma_k \mu_T) \frac{\partial k}{\partial x_3} \right), \end{aligned} \quad (2)$$

$$\begin{aligned} \frac{\partial \rho \omega}{\partial t} + \frac{\partial \rho \omega v_1}{\partial x_1} + \frac{\partial \rho \omega v_2}{\partial x_2} + \frac{\partial \rho \omega v_3}{\partial x_3} &= P_\omega - \beta \rho \omega \omega + C_D + \frac{\partial}{\partial x_1} \left((\mu + \sigma_\omega \mu_T) \frac{\partial \omega}{\partial x_1} \right) + \\ &+ \frac{\partial}{\partial x_2} \left((\mu + \sigma_\omega \mu_T) \frac{\partial \omega}{\partial x_2} \right) + \frac{\partial}{\partial x_3} \left((\mu + \sigma_\omega \mu_T) \frac{\partial \omega}{\partial x_3} \right), \end{aligned} \quad (3)$$

where k the turbulent kinetic energy and ω the turbulent dissipation are functions of time t and space coordinates x_1, x_2, x_3 . The production terms P_k and P_ω are given by formulas

$$P_k = \tau_{11} \frac{\partial v_1}{\partial x_1} + \tau_{12} \frac{\partial v_1}{\partial x_2} + \tau_{21} \frac{\partial v_2}{\partial x_1} + \tau_{22} \frac{\partial v_2}{\partial x_2} + \tau_{13} \frac{\partial v_1}{\partial x_3} + \tau_{31} \frac{\partial v_3}{\partial x_1} + \tau_{23} \frac{\partial v_2}{\partial x_3} + \tau_{32} \frac{\partial v_3}{\partial x_2} + \tau_{33} \frac{\partial v_3}{\partial x_3},$$

where functions τ are defined in (1) with $\mu = 0$.

$$P_\omega = \frac{\alpha_\omega \omega P_k}{k}, \text{ where } \alpha_\omega = \frac{\beta}{\beta^*} - \frac{\sigma_\omega \kappa^2}{\sqrt{\beta^*}} \text{ and } \sigma_k = \frac{2}{3}, \beta^* = 0.09, \beta = \frac{5}{6} \beta^*, \sigma_\omega = 0.5, \kappa = 0.41.$$

The cross-diffusion term C_D is defined as $C_D = \sigma_d \frac{\rho}{\omega} \max \left\{ \frac{\partial k}{\partial x_1} \frac{\partial \omega}{\partial x_1} + \frac{\partial k}{\partial x_2} \frac{\partial \omega}{\partial x_2} + \frac{\partial k}{\partial x_3} \frac{\partial \omega}{\partial x_3}, 0 \right\}$, where $\sigma_d = 0.5$ is constant.

We assume that the partial derivatives exist, such that the differential formulation (1) makes sense. Within the numerical solution of this problem (1),(2),(3) we usually consider the equations in the more general integral form, which allows the discontinuities in the solution. It is well known that the classical Navier-Stokes equation for three-dimensional incompressible viscous flow is invariant under Galilean transformations, see (Feistauer, 1993, page 69). We can choose a new Cartesian coordinate system $(\tilde{x}_1, \tilde{x}_2, \tilde{x}_3)$ with the origin is at the point $\tilde{\sigma}$, we write

$$\begin{pmatrix} \tilde{x}_1 \\ \tilde{x}_2 \\ \tilde{x}_3 \end{pmatrix} = \mathbb{Q}_0 \begin{pmatrix} x_1 \\ x_2 \\ x_3 \end{pmatrix} + \tilde{\sigma}, \text{ with } \mathbb{Q}_0 = \begin{pmatrix} \mathbf{n} \\ \mathbf{o} \\ \mathbf{p} \end{pmatrix} = \begin{pmatrix} n_1 & n_2 & n_3 \\ o_1 & o_2 & o_3 \\ p_1 & p_2 & p_3 \end{pmatrix}. \quad (4)$$

The transformation of the state vector \mathbf{w} yields the state vector \mathbf{q} in the new coordinates

$$\begin{aligned} \mathbf{q} &= \mathbb{Q} \mathbf{w}, \\ \mathbf{w} &= \mathbb{Q}^{-1} \mathbf{q}, \end{aligned} \quad \mathbb{Q} = \begin{pmatrix} 1 & 0 & 0 & 0 & 0 \\ 0 & n_1 & n_2 & n_3 & 0 \\ 0 & o_1 & o_2 & o_3 & 0 \\ 0 & p_1 & p_2 & p_3 & 0 \\ 0 & 0 & 0 & 0 & 1 \end{pmatrix}, \quad \mathbb{Q}^{-1} = \begin{pmatrix} 1 & 0 & 0 & 0 & 0 \\ 0 & n_1 & o_1 & p_1 & 0 \\ 0 & n_2 & o_2 & p_2 & 0 \\ 0 & n_3 & o_3 & p_3 & 0 \\ 0 & 0 & 0 & 0 & 1 \end{pmatrix}. \quad (5)$$

The vectors $\mathbf{n}, \mathbf{o}, \mathbf{p}$ must have the properties $|\mathbf{n}| = |\mathbf{o}| = 1$, $\mathbf{n} \cdot \mathbf{o} = 0$, $\mathbf{p} = \mathbf{n} \times \mathbf{o}$. We can choose the vector $\mathbf{o} = (o_1, o_2, o_3)$ such that $\mathbf{n} \cdot \mathbf{o} = 0$, $|\mathbf{o}| = 1$. And then the vector $\mathbf{p} = (p_1, p_2, p_3)$ is determined by $\mathbf{p} = \mathbf{n} \times \mathbf{o}$. The axis \tilde{x}_2 points in the direction of the vector \mathbf{o} , and the axis \tilde{x}_3 in the direction of the vector \mathbf{p} .

The Euler Equations

Ommiting the viscous terms in (1) we get the system of the Euler equations

$$\frac{\partial \mathbf{w}}{\partial t} + \sum_{s=1}^3 \frac{\partial \mathbf{f}_s(\mathbf{w})}{\partial x_s} = 0 \quad \text{in } Q_T = \Omega \times (0, T). \quad (6)$$

The equations (6) represent a system of hyperbolic partial differential equations. The system of the Euler equations is rotationally invariant (see e.g. (Feistauer, 2003, page 108)).

3. FVM discretization of the problem

According to (Wilcox, 1998, page 365), the coupling between the turbulence-model equations (2),(3) and the mean-flow equations appears to be relatively weak. Therefore we solve the systems sequentially. Here we describe the so-called *finite volume* discretization of the system (1) in the domain Ω , the discretization of the system (2),(3) can be done analogically, see Kyncl, Pelant (2012). By Ω_h let us denote the polyhedral approximation of Ω . The system of the closed polyhedrons with mutually disjoint interiors $\mathcal{D}_h = \{D_i\}_{i \in J}$, where $J \subset \mathbb{Z}^+ = \{0, 1, \dots\}$ is an index set and $h > 0$, will be called a *finite volume mesh*. This system \mathcal{D}_h approximates the domain Ω , we write $\bar{\Omega}_h = \bigcup_{i \in J} D_i$. The elements $D_i \in \mathcal{D}_h$ are called the *finite volumes*. For two neighboring elements D_i, D_j we set $\Gamma_{ij} = \partial D_i \cap \partial D_j = \Gamma_{ji}$. Here we will work with the so-called *regular* meshes, i.e. the intersection of two arbitrary (different) elements is either empty or it consists of a common vertex or a common edge or a common face (in 3D). The boundary ∂D_i of each element D_i is $\partial D_i = \bigcup_{\Gamma_{ij} \in \Gamma_{D_i}} \Gamma_{ij}$. Here the set $\Gamma_{D_i} = \{\Gamma_{ij}; \Gamma_{ij} \subset \partial D_i\}$ forms the boundary ∂D_i . By \mathbf{n}_{ij} let us denote the unit outer normal to ∂D_i on Γ_{ij} . Let us construct a partition $0 = t_0 < t_1 < \dots$ of the time interval $[0, T]$ and denote the time steps $\tau_k = t_{k+1} - t_k$. We integrate the system (1) over the set $D_i \times (t_k, t_{k+1})$. With the integral form of the equations we can study a flow with discontinuities, such as shock waves, too.

$$\int_{D_i} \int_{t_k}^{t_{k+1}} \frac{\partial \mathbf{w}}{\partial t} dx dt + \int_{t_k}^{t_{k+1}} \int_{D_i} \sum_{s=1}^3 \frac{\partial \mathbf{f}_s(\mathbf{w})}{\partial x_s} dx dt = \int_{t_k}^{t_{k+1}} \int_{D_i} \sum_{s=1}^3 \frac{\partial \mathcal{R}_s(\mathbf{w}, \nabla \mathbf{w})}{\partial x_s} dx dt \quad (7)$$

Using the Green's theorem on D_i it is

$$\int_{D_i} \sum_{s=1}^3 \frac{\partial \mathbf{f}_s(\mathbf{w})}{\partial x_s} dx = \int_{\partial D_i} \sum_{s=1}^3 \mathbf{f}_s(\mathbf{w}) n_s dS, \quad \int_{D_i} \sum_{s=1}^3 \frac{\partial \mathcal{R}_s(\mathbf{w}, \nabla \mathbf{w})}{\partial x_s} dx = \int_{\partial D_i} \sum_{s=1}^3 \mathcal{R}_s(\mathbf{w}, \nabla \mathbf{w}) n_s dS.$$

Here $\mathbf{n} = (n_1, n_2, n_3)$ is the unit outer normal to ∂D_i . Further we rewrite (7)

$$\int_{D_i} (\mathbf{w}(x, t_{k+1}) - \mathbf{w}(x, t_k)) dx + \int_{t_k}^{t_{k+1}} \sum_{\Gamma_{ij} \in \Gamma_{D_i}} \int_{\Gamma_{ij}} \sum_{s=1}^3 (\mathbf{f}_s(\mathbf{w}) - \mathcal{R}_s(\mathbf{w}, \nabla \mathbf{w})) (n_{ij})_s dS dt = 0 \quad (8)$$

We define a finite volume approximate solution of the system studied (1) as a piecewise constant vector-valued functions \mathbf{w}_h^k , $k = 0, 1, \dots$, where \mathbf{w}_h^k is constant on each element D_i , and t_k is the time instant. By \mathbf{w}_i^k we denote the value of the approximate solution on D_i at time t_k . We approximate the integral over the element D_i as $\int_{D_i} \mathbf{w}(x, t_k) dx \approx |D_i| \mathbf{w}_i^k$. Further we proceed with the approximation of the fluxes. Here we show the numerical flux based on the solution of the Riemann problem for the split Euler equations (shown later in Section 4.). By $\mathbf{w}_{\Gamma_{ij}}^l$ let us

denote the state vector \mathbf{w} at the center of the edge Γ_{ij} at the time instant t_l , and let us suppose $\mathbf{w}_{\Gamma_{ij}}^l$ is known. Evaluation of these values will be a question of the further analysis, here we use them to approximate the integrals with the one-point rule

$$\int_{\Gamma_{ij}} \sum_{s=1}^3 \mathbf{f}_s(\mathbf{w}(x, t_l))(n_{ij})_s dS \approx |\Gamma_{ij}| \sum_{s=1}^3 \mathbf{f}_s(\mathbf{w}_{\Gamma_{ij}}^l)(n_{ij})_s. \quad (9)$$

$$\int_{\Gamma_{ij}} \sum_{s=1}^3 \mathbb{R}_s(\mathbf{w}(x, t_l), \nabla \mathbf{w}(x, t_l))(n_{ij})_s dS \approx |\Gamma_{ij}| \sum_{s=1}^3 \mathbb{R}_s(\mathbf{w}_{\Gamma_{ij}}^l, \nabla \mathbf{w}_{\Gamma_{ij}}^l)(n_{ij})_s.$$

Here $\nabla \mathbf{w}_{\Gamma_{ij}}^l$ denotes the $\nabla \mathbf{w}$ at the center of the edge Γ_{ij} at time instant t_l . Now it is possible to approximate the system (8) by the following **explicit finite volume scheme**

$$|D_i|(\mathbf{w}_i^{k+1} - \mathbf{w}_i^k) + \tau_k \sum_{\Gamma_{ij} \in \Gamma_{D_i}} |\Gamma_{ij}| \sum_{s=1}^3 \left(\mathbf{f}_s(\mathbf{w}_{\Gamma_{ij}}^k) n_s - \mathbb{R}_s(\mathbf{w}_{\Gamma_{ij}}^k, \nabla \mathbf{w}_{\Gamma_{ij}}^k) n_s \right) = 0 \quad (10)$$

With this finite volume formula one computes the values of the approximate solution at the time instant t_{k+1} , using the values from the time instant t_k , and by evaluating the values $\mathbf{w}_{\Gamma_{ij}}^k$ at the faces Γ_{ij} . In order to achieve the stability of the used method, the time step τ_k must be restricted by the so-called CFL condition, see Feistauer (2003). The crucial problem of this discretization lies with the **evaluation of the face values** $\mathbf{w}_{\Gamma_{ij}}^k$ and its spatial derivatives $\nabla \mathbf{w}_{\Gamma_{ij}}^k$. Or one deals with the problem of finding the face fluxes $\mathbf{H}(\mathbf{w}_i^k, \mathbf{w}_j^k, \mathbf{n}_{ij})$. Here, for the simplicity, we work with the explicit scheme. The discretization via the implicit scheme can be found in Kyncl, Pelant (2012). Further (Section 3.1.) we show the **discretization of the face values**, which is the aim of this paper. For the discretization of the spatial derivatives it is possible to use the procedure shown in Kyncl, Pelant (2012).

Let us show the approximation of these spatial derivatives on the function denoted by $f = f(x)$. The values of the function f on each element D_i are known. We approximate the values of this function at all mesh points P_j as the weighted average over all volumes D_i with vertex P_j

$$f(P_j) = \frac{\sum_{D_i; P_j \in \partial D_i} f|_{D_i} |D_i|}{\sum_{D_i; P_j \in \partial D_i} |D_i|}.$$

By the notation $\sum_{D_i; P_j \in \partial D_i}$ we mean the summation over all volumes D_i with the vertex P_j , and by $|D_i|$ we denote the volume of the element D_i . Further we apply the boundary condition for $f(P_j)$ at the points P_j , laying on the boundary of the studied area. For example we prescribe the zero velocity and given temperature at the points laying on the boundary segment representing the wall. Now let us choose a face Γ_{ij} . The values of the function f are known at its vertices P_m , and at the centers C_I, C_J of the adjacent elements D_i, D_j . It is possible to use n-point rule to approximate the spatial derivatives of the function f at the face Γ_{ij} . For the face with m vertices, it is possible to use the $m + 2$ point rule (the face vertices P_l are numbered counter-clockwise, looking from C_J)

$$\overrightarrow{\nabla} f = \frac{1}{|K|} \left\{ \overrightarrow{\mathbf{n}}_{ij} |\Gamma_{ij}| (f(C_J) - f(C_I)) + \sum_{l=1}^m f(P_l) \frac{\overrightarrow{P_l - P_{l+}} \times \overrightarrow{C_I C_J}}{2} \right\}. \quad (11)$$

Here $l^- = \begin{cases} l-1, & l > 1 \\ m, & l = 1 \end{cases}$, $l^+ = \begin{cases} l+1, & l < m \\ 1, & l = m \end{cases}$, and $|K| = |\Gamma_{ij}| (\overrightarrow{\mathbf{n}}_{ij} \cdot \overrightarrow{C_I C_J})$.

At the boundary face Γ , where the function f is given by the value $f(\Gamma)$, the ∇f can be approximated as

$$\overrightarrow{\nabla f} = \frac{1}{h} (f(\Gamma) - f(C_I)) \overrightarrow{\mathbf{n}}, \quad h = \overrightarrow{\mathbf{n}} \cdot \overrightarrow{C_I C_\Gamma},$$

with h being the distance of the volume center C_I to the face Γ , C_Γ is the center of the face Γ .

3.1. Face values / Euler fluxes discretization

To approximate the face values $\mathbf{w}_{\Gamma_{ij}}^k$ at time instant t_k we solve the simplified system (12) in the vicinity of the face Γ_{ij} in time with the initial condition formed by the state vectors \mathbf{w}_i^k and \mathbf{w}_j^k . Using the rotational invariance of the Euler equations, the system (6) is expressed in a new Cartesian coordinate system $\tilde{x}_1, \tilde{x}_2, \tilde{x}_3$ with the origin at the center of the gravity of Γ_{ij} and with the new axis \tilde{x}_1 in the direction of $\mathbf{n} = (n_1, n_2, n_3)$, given by the face normal $\mathbf{n} = \mathbf{n}_{ij}$.



Figure 1: Coordinate transformation for the inner and boundary edges in 2D (inner edge left).

Then the derivatives with respect to \tilde{x}_2, \tilde{x}_3 are neglected and we get the so-called split 3D Euler equations, see (Feistauer, 2003, page 138):

$$\frac{\partial \mathbf{q}}{\partial t} + \frac{\partial \mathbf{f}_1(\mathbf{q})}{\partial \tilde{x}_1} = 0. \quad (12)$$

The values \mathbf{w}_i^k and \mathbf{w}_j^k adjacent to the face Γ_{ij} are known, forming the initial conditions

$$\mathbf{q}(\tilde{x}_1, 0) = \mathbf{q}_L = \mathbb{Q} \mathbf{w}_i^k, \quad \tilde{x}_1 < 0, \quad (13)$$

$$\mathbf{q}(\tilde{x}_1, 0) = \mathbf{q}_R = \mathbb{Q} \mathbf{w}_j^k, \quad \tilde{x}_1 > 0. \quad (14)$$

The transformation matrix \mathbb{Q} is defined in (5). In this work we will refer to these initial conditions as to the left-hand side initial condition (13) and the right-hand side initial condition (14). The problem (12), (13), (14) has a unique “solution” in $(-\infty, \infty) \times (0, \infty)$, the analysis can be found in (Feistauer, 2003, page 138), we will show the analysis of this problem later in Section 4.. Let $\mathbf{q}_{RS}(\mathbf{q}_L, \mathbf{q}_R, \tilde{x}_1, t)$ denote the solution of this problem at the point (\tilde{x}_1, t) . We are interested in the solution of this local problem at the time axis, which is the sought solution in the local coordinates $\mathbf{q}_{\Gamma_{ij}} = \mathbf{q}_{RS}(\mathbf{q}_L, \mathbf{q}_R, 0, t)$. The backward transformation (5) of the state vector $\mathbf{q}_{\Gamma_{ij}}$ into the global coordinates is $\mathbf{w}_{\Gamma_{ij}}^k = \mathbb{Q}^{-1} \mathbf{q}_{\Gamma_{ij}} = \mathbb{Q}^{-1} \mathbf{q}_{RS}(\mathbb{Q} \mathbf{w}_i^k, \mathbb{Q} \mathbf{w}_j^k, 0, t)$. The described process of finding the face values $\mathbf{w}_{\Gamma_{ij}}^k$ is independent on the choice of the vectors \mathbf{o}, \mathbf{p} , determining the transformation matrix \mathbb{Q} defined in (5), see Kyncl (2011).

At the boundary faces (edges) we work with the problem (12) equipped with only one-side initial condition (13). The problem of the **boundary condition** is to choose the **boundary state**

$$\mathbf{q}(0, t) = \mathbf{q}_B, \quad t > 0. \quad (15)$$

such a way that the system (12),(13),(15) is well-posed, i.e. it has a unique solution (entropy weak) in the considered set $\Omega_B = \{(\tilde{x}_1, t); \tilde{x}_1 \leq 0, t > 0\}$. It is possible to show, that by adding properly chosen equations into the system (12),(13) it is possible to reconstruct the boundary state \mathbf{q}_B such that the system (12),(13),(15) has a unique solution in Ω_B , see Kyncl (2011). We will refer to these added equations as to **complementary conditions**. Several choices of the complementary conditions will be discussed further.

4. The Riemann problem for the split Euler equations

For many numerical methods dealing with the two or three dimensional equations, describing the compressible flow, it is useful to solve the *split* Riemann problem. Here we will follow in 3D, analogously it is possible to proceed in 2D. It is the system of the equations (12), equipped with the initial conditions (13),(14)

$$\frac{\partial \mathbf{q}}{\partial t} + \frac{\partial \mathbf{f}_1(\mathbf{q})}{\partial \tilde{x}_1} = 0, \quad \mathbf{q}(\tilde{x}_1, 0) = \begin{cases} \mathbf{q}_L, & \tilde{x}_1 < 0, \\ \mathbf{q}_R, & \tilde{x}_1 > 0. \end{cases}$$

‘Split’ means here that we still have 5 equations in 3D, but the dependence on \tilde{x}_2, \tilde{x}_3 is neglected, and we deal with the system for one space variable \tilde{x}_1 . The system (12) is considered in the set $Q_\infty = (-\infty, \infty) \times (0, +\infty)$. The solution of this simplified system is useful when dealing with the inviscid fluxes within various numerical methods.

The solution of this problem is fundamentally the same as the solution of the Riemann problem for the 1D Euler equations, see (Feistauer, 2003, page 138). In fact, the solution for the pressure, the first component of the velocity, and the density is exactly the same as in one-dimensional case. It is a characteristic feature of the hyperbolic equations, that there is a possible raise of discontinuities in solutions, even in the case when the initial conditions are smooth, see (Feistauer, 1993, page 390). Here the concept of the classical solution is too restrictive, and therefore we seek a weak solution of this problem. To distinguish physically admissible solutions from nonphysical ones, entropy condition must be introduced, see (Feistauer, 1993, page 396). By the solution of the problem (12),(13),(14) we mean the *weak entropy solution* of this problem in Q_∞ . The analysis to the solution of this problem can be found in many books, i.e. Feistauer (2003), Feistauer (1993), TORO (1997). The general theorem on the solvability of the Riemann problem can be found in (Feistauer, 2003, page 88). Here we summarize, that the problem has a unique solution for certain choice of the initial conditions. This solution can be written for $t > 0$ in the similarity form $\mathbf{q}(\tilde{x}_1, t) = \tilde{\mathbf{q}}(\tilde{x}_1/t)$, where $\tilde{\mathbf{q}}(\tilde{x}_1/t) : \mathbb{R} \rightarrow \mathbb{R}^3$ ((Feistauer, 2003, page 82)). Now we will show the form of the possible solution $\mathbf{q} = \mathbf{q}(\tilde{x}_1, t)$ of the Riemann problem (12),(13),(14). The solution is piecewise **smooth** and its general form can be seen in Fig. 2, where the system of half lines is drawn. These half lines define regions, where \mathbf{q} is either constant or given by a smooth function. Let us define the open sets called **wedges** $\Omega_L, \Omega_{HTL}, \Omega_{*L}, \Omega_{*R}, \Omega_{HTR}, \Omega_R$, see Fig. 2. We will refer to the set Ω_{HTL} as to the left wave, and the set Ω_{HTR} will be called the right wave. The solution in $\Omega_L, \Omega_{*L}, \Omega_{*R}, \Omega_R$ is constant (see e.g. (Feistauer, 2003, page 128)), while in Ω_{HTL} and in Ω_{HTR} it is continuous. Let us denote $\mathbf{q}|_{\Omega_L} = \mathbf{q}_L, \mathbf{q}|_{\Omega_{*L}} = \mathbf{q}_{*L}, \mathbf{q}|_{\Omega_{*R}} = \mathbf{q}_{*R}, \mathbf{q}|_{\Omega_R} = \mathbf{q}_R, \mathbf{q}|_{\Omega_{HTL}} = \mathbf{q}_{HTL}, \mathbf{q}|_{\Omega_{HTR}} = \mathbf{q}_{HTR}$.

It is more convenient to use the vector of primitive variables (ϱ, u, v, w, p) rather than the vector of conservative variables $(\varrho, \varrho u, \varrho v, \varrho w, E)$ in solving the Riemann problem. The exact solution of the Riemann problem has three waves in general, illustrated in Fig. 2. The wedges Ω_L and Ω_{*L} are separated by the left wave (either 1-*shock wave*, or 1-*rarefaction wave*). There is a

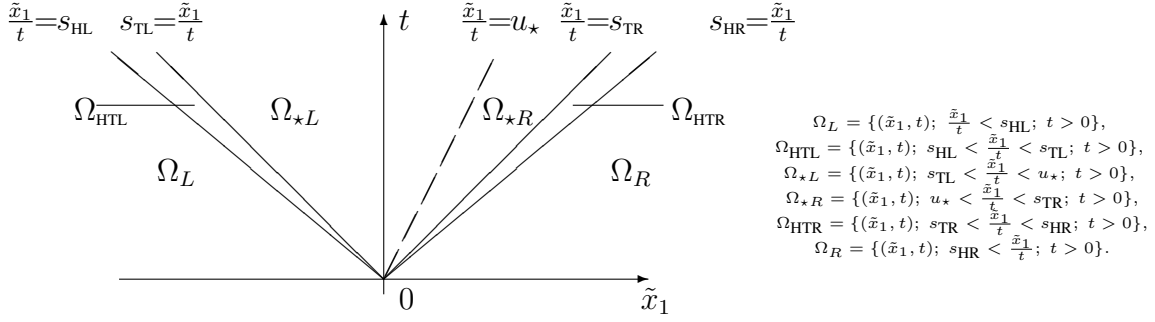


Figure 2: Structure of the solution of the Riemann problem (12),(13),(14)

contact discontinuity between the regions Ω_{*L} and Ω_{*R} . Wedges Ω_{*R} and Ω_R are separated by the right wave (either 3-shock wave, or 3-rarefaction wave). The solution for the primitive variables can be described as follows:

$$\begin{aligned}
(\varrho, u, v, w, p)|_{\Omega_L} &= (\varrho_L, u_L, v_L, w_L, p_L), & (\varrho, u, v, w, p)|_{\Omega_{*R}} &= (\varrho_{*R}, u_*, v_R, w_R, p_*), \\
(\varrho, u, v, w, p)|_{\Omega_{*L}} &= (\varrho_{*L}, u_*, v_L, w_L, p_*), & (\varrho, u, v, w, p)|_{\Omega_R} &= (\varrho_R, u_R, v_R, w_R, p_R).
\end{aligned}$$

The following relations for these variables hold:

$$u_* = u_L + \begin{cases} -(p_* - p_L) \left(\frac{2}{p_* + \frac{\gamma-1}{\gamma+1} p_L} \right)^{\frac{1}{2}}, & p_* > p_L \\ \frac{2}{\gamma-1} a_L \left[1 - \left(\frac{p_*}{p_L} \right)^{(\gamma-1)/2\gamma} \right], & p_* \leq p_L \end{cases} \quad (16) \quad u_* = u_R + \begin{cases} (p_* - p_R) \left(\frac{2}{p_* + \frac{\gamma-1}{\gamma+1} p_R} \right)^{\frac{1}{2}}, & p_* > p_R \\ -\frac{2}{\gamma-1} a_R \left[1 - \left(\frac{p_*}{p_R} \right)^{(\gamma-1)/2\gamma} \right], & p_* \leq p_R \end{cases} \quad (19)$$

$$\varrho_{*L} = \begin{cases} \varrho_L \frac{\frac{\gamma-1}{\gamma+1} \frac{p_L}{p_*} + 1}{\frac{p_L}{p_*} + \frac{\gamma-1}{\gamma+1}}, & p_* > p_L \\ \varrho_L \left(\frac{p_*}{p_L} \right)^{\frac{1}{\gamma}}, & p_* \leq p_L \end{cases} \quad (17) \quad \varrho_{*R} = \begin{cases} \varrho_R \frac{\frac{p_*}{p_R} + \frac{\gamma-1}{\gamma+1}}{\frac{\gamma-1}{\gamma+1} \frac{p_*}{p_R} + 1}, & p_* > p_R \\ \varrho_R \left(\frac{p_*}{p_R} \right)^{\frac{1}{\gamma}}, & p_* \leq p_R \end{cases} \quad (20)$$

$$s_{TL}^1 = \begin{cases} u_L - a_L \sqrt{\frac{\gamma+1}{2\gamma} \frac{p_*}{p_L} + \frac{\gamma-1}{2\gamma}}, & p_* > p_L \\ u_* - a_L \left(\frac{p_*}{p_L} \right)^{\frac{1}{2\gamma}}, & p_* \leq p_L \end{cases} \quad (18) \quad s_{TR}^3 = \begin{cases} u_R + a_R \sqrt{\frac{\gamma+1}{2\gamma} \frac{p_*}{p_R} + \frac{\gamma-1}{2\gamma}}, & p_* > p_R \\ u_* + a_R \left(\frac{p_*}{p_R} \right)^{\frac{1}{2\gamma}}, & p_* \leq p_R \end{cases} \quad (21)$$

Here $a_L = \sqrt{\gamma p_L / \varrho_L}$, $a_R = \sqrt{\gamma p_R / \varrho_R}$, and γ denotes the adiabatic constant. Further s_{TL}^1 denotes "unknown left wave speed", s_{TR}^3 "unknown right wave speed". Note, that the system (16) - (21) is the system of 6 equations for 6 unknowns $p_*, u_*, \varrho_{*L}, \varrho_{*R}, s_{TL}^1, s_{TR}^3$. The solution of this system leads to a nonlinear algebraic equation, and one cannot express the analytical solution of this problem in a closed form. The problem has a solution only if the *pressure positivity condition* is satisfied

$$u_R - u_L < \frac{2}{\gamma-1} (a_L + a_R). \quad (22)$$

We will use some of these relations to construct and solve the initial-boundary value problem which will be the original result of our work.

Remarks

- Once the pressure p_* is known, the solution on the left-hand side of the contact discontinuity depends only on the left-hand side initial condition (13). And similarly, with p_* known, only the right-hand side initial condition (14) is used to compute the solution on the right-hand side of the contact discontinuity.

- The solution in $\Omega_L \cup \Omega_{HTL} \cup \Omega_{*L}$ (across 1 wave)
 There are three unknowns in the region Ω_{*L} . It is the density ρ_{*L} , the pressure p_* , and the velocity u_* . Also the speed s_{TL}^1 of the left wave determining the position of the region Ω_{HTL} is not known. The solution components in $\Omega_L \cup \Omega_{HTL} \cup \Omega_{*L}$ region must satisfy the system of equations (16)-(18). It is a system of three equations for four unknowns. We have to add another equation in order to get the uniquely solvable system in $\Omega_L \cup \Omega_{HTL} \cup \Omega_{*L}$.

5. Boundary condition by preference of pressure

In this section we construct the boundary condition, i.e. the state q_B in (15), preferring the given value for the pressure $p_{GIVEN} > 0$. This boundary condition corresponds to the real-world problem, when we deal with the experimentally obtained pressure distribution at the boundary. We add the following **complementary conditions** into the system (12),(13)

$$p_* := p_{GIVEN}, p_R = p_*, \rho_{*R} := \rho_{GIVEN}, v_R := v_{GIVEN}, w_R := w_{GIVEN}. \quad (23)$$

Here p_* is the pressure in $\Omega_{*L} \cup \Omega_{*R}$, see Section 4.. The conditions (23) prescribe the given pressure wherever it is possible, solution in Ω_L is governed by the condition (13). We seek the **boundary state** q_B as the unique solution of the problem (12),(13),(23) at the half line $S_B = \{(0, t); t > 0\}$. The system (16)-(21), (23) is uniquely solvable. The algorithm for the construction of the primitive variables $\rho_B, u_B, v_B, w_B, p_B$ at the half-line S_B is shown in Fig. 3. The complete analysis of this problem is shown in Kyncl (2011).

$p_* > p_L$			$p_* \leq p_L$			
$s_1 = u_L - \sqrt{\gamma \frac{p_L}{\rho_L}} \sqrt{\frac{\gamma+1}{2\gamma} \frac{p_*}{p_L} + \frac{\gamma-1}{2\gamma}}$ $u_* = u_L - (p_* - p_L) \left(\frac{\frac{2}{(\gamma+1)\rho_L}}{p_* + \frac{\gamma-1}{\gamma+1} p_L} \right)^{\frac{1}{2}}$ $\rho_{*L} = \rho_L \frac{\frac{\gamma-1}{\gamma+1} \frac{p_L}{p_*} + 1}{\frac{p_L}{p_*} + \frac{\gamma-1}{\gamma+1}}$			$a_L = \sqrt{\gamma \frac{p_L}{\rho_L}}, \quad s_{HL} = u_L - a_L$ $u_* = u_L + \frac{2}{\gamma-1} a_L \left(1 - \left(\frac{p_*}{p_L} \right)^{(\gamma-1)/2\gamma} \right)$ $s_{TL} = u_* - a_L \left(\frac{p_*}{p_L} \right)^{(\gamma-1)/2\gamma}$ $\rho_{*L} = \rho_L \left(\frac{p_*}{p_L} \right)^{1/\gamma}$			
$s_1 > 0$	$s_1 \leq 0$		$s_{HL} \geq 0$	$s_{TL} \geq 0$	$s_{HL} < 0$	$s_{TL} < 0$
	$u_* \geq 0$	$u_* < 0$			$u_* \geq 0$	$u_* < 0$
<p>OUTLET</p> $p_B = p_L$ $u_B = u_L$ $v_B = v_L$ $w_B = w_L$ $\rho_B = \rho_L$	<p>OUTLET</p> $p_B = p_*$ $u_B = u_*$ $v_B = v_L$ $w_B = w_L$ $\rho_B = \rho_{*L}$	<p>INLET</p> $p_B = p_*$ $u_B = u_*$ $v_B = v_R$ $w_B = w_R$ $\rho_B = \rho_{*R}$	<p>OUTLET</p> $p_B = p_L$ $u_B = u_L$ $v_B = v_L$ $w_B = w_L$ $\rho_B = \rho_L$	<p>OUTLET</p> $\tau_\theta = \theta \theta$ $\tau_d = \theta d$ $\tau_m = \theta m$ $\tau_n = \theta n$ $\tau_o = \theta o$	<p>OUTLET</p> $p_B = p_*$ $u_B = u_*$ $v_B = v_L$ $w_B = w_L$ $\rho_B = \rho_{*L}$	<p>INLET</p> $p_B = p_*$ $u_B = u_*$ $v_B = v_R$ $w_B = w_R$ $\rho_B = \rho_{*R}$

Figure 3: Boundary condition by preference of pressure, algorithm for the solution at the boundary. The value of the pressure p_* is prescribed, solution $\rho_B, u_B, v_B, w_B, p_B$ is computed.

6. Boundary condition by preference of velocity

In this section we construct the boundary condition, i.e. the state \mathbf{q}_B in (15), preferring the given value for the velocity u_{GIVEN} . We add the following **complementary conditions** into the system (12),(13)

$$u_\star := u_{\text{GIVEN}}, u_R = u_\star, \varrho_{\star R} := \varrho_{\text{GIVEN}}, v_R := v_{\text{GIVEN}}, w_R := w_{\text{GIVEN}}. \quad (24)$$

We seek the **boundary state** \mathbf{q}_B as the unique solution of the problem (12),(13),(24) at the half line $S_B = \{(0, t); t > 0\}$. The system (16)-(21), (24) is uniquely solvable. The algorithm for the construction of the primitive variables $\varrho_B, u_B, v_B, w_B, p_B$ at the half-line S_B is shown in Fig. 4. The complete analysis of this problem is shown in Kyncl (2011).

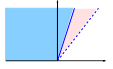
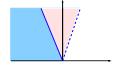
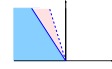
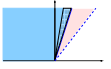
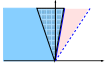
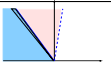
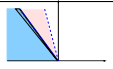
$u_\star < u_L$			$u_\star \geq u_L$			
$D = 4\varrho_L \gamma p_L + \varrho_L^2 \left(\frac{\gamma+1}{2}\right)^2 (u_L - u_\star)^2$ $p_\star = \frac{1}{2} \left(2p_L + \frac{\gamma-1}{2} \varrho_L (u_L - u_\star)^2 + (u_L - u_\star) \sqrt{D} \right)$ $s_1 = u_L - \sqrt{\gamma \frac{\varrho_L}{\varrho_\star} \sqrt{\frac{\gamma+1}{2\gamma} \frac{p_\star}{p_L} + \frac{\gamma-1}{2\gamma}}}$ $\varrho_{\star L} = \varrho_L \frac{\frac{\gamma-1}{\gamma+1} \frac{p_L}{p_\star} + 1}{\frac{p_L}{p_\star} + \frac{\gamma-1}{\gamma+1}}$			$a_L = \sqrt{\gamma \frac{p_L}{\varrho_L}}, \quad s_{HL} = u_L - a_L$ $p_\star = p_L \left(\frac{-u_\star + u_L + \frac{2}{\gamma-1} a_L}{\frac{2}{\gamma-1} a_L} \right)^{\frac{2\gamma}{\gamma-1}}$ $s_{TL} = u_\star - a_L \left(\frac{p_\star}{p_L} \right)^{(\gamma-1)/2\gamma}$ $\varrho_{\star L} = \varrho_L \left(\frac{p_\star}{p_L} \right)^{1/\gamma}$			
$s_1 \geq 0$	$s_1 < 0$		$s_{HL} \geq 0$	$s_{HL} < 0$		
	$u_\star \geq 0$	$u_\star < 0$		$s_{TL} \geq 0$	$u_\star \geq 0$	$s_{TL} < 0$
 <p>OUTLET</p> $p_B = p_L$ $u_B = u_L$ $v_B = v_L$ $w_B = w_L$ $\varrho := \varrho_L$	 <p>OUTLET</p> $p_B = p_\star$ $u_B = u_\star$ $v_B = v_L$ $w_B = w_L$ $\varrho_B = \varrho_{\star L}$	 <p>INLET</p> $p_B = p_\star$ $u_B = u_\star$ $v_B = v_R$ $w_B = w_R$ $\varrho_B = \varrho_{\star R}$	 <p>OUTLET</p> $p_B = p_L$ $u_B = u_L$ $v_B = v_L$ $w_B = w_L$ $\varrho_B = \varrho_L$	 <p>OUTLET</p> $p_B = p_L$ $u_B = \frac{\gamma+1}{2} \left[\frac{2}{\gamma+1} + \frac{\gamma-1}{2} \frac{\varrho_B}{\varrho_L} \right]$ $v_B = \frac{\gamma+1}{2} \left[\frac{2}{\gamma+1} + \frac{\gamma-1}{2} \frac{\varrho_B}{\varrho_L} \right]$ $w_B = \frac{\gamma+1}{2} \left[\frac{2}{\gamma+1} + \frac{\gamma-1}{2} \frac{\varrho_B}{\varrho_L} \right]$ $\varrho_B = \varrho_L \left(\frac{p_B}{p_L} \right)^{1/\gamma}$	 <p>OUTLET</p> $p_B = p_\star$ $u_B = u_\star$ $v_B = v_L$ $w_B = w_L$ $\varrho_B = \varrho_{\star L}$	 <p>INLET</p> $p_B = p_\star$ $u_B = u_\star$ $v_B = v_R$ $w_B = w_R$ $\varrho_B = \varrho_{\star R}$

Figure 4: Algorithm for the solution of the problem (12),(13),(24) at the half line $S_B = \{(0, t); t > 0\}$. Possible situations are illustrated by the pictures showing the region $\Omega_L \cup \Omega_{HTL} \cup \Omega_{\star L}$ with the sought boundary state located at the time axis.

6.1. B.C. for the Impermeable Wall

As a special case of the complementary condition (24) we prescribe zero normal velocity, i.e. we choose $u_\star := 0$. Using the analysis in Section 6. we construct the solution of the system

(12),(13),(24) in primitive variables. It is

$$\begin{pmatrix} \varrho_B \\ u_B \\ v_B \\ w_B \\ p_B \end{pmatrix} = \begin{cases} \begin{pmatrix} \frac{\varrho_L}{\frac{\gamma+1}{2} \frac{p_*}{p_* + \gamma+1}} \\ 0 \\ v_L \\ w_L \\ p_* \end{pmatrix}, & \text{with } p_* = \frac{2p_L + \frac{\gamma+1}{2} \varrho_L u_L^2 + u_L \sqrt{4\varrho_L \gamma p_L + \varrho_L^2 (\frac{\gamma+1}{2})^2 u_L^2}}{2}, \quad u_L > 0, \\ \begin{pmatrix} \varrho_L \left(1 + \frac{\gamma-1}{2} \frac{u_L}{a_L}\right)^{\frac{2}{\gamma-1}} \\ 0 \\ v_L \\ w_L \\ p_L \left(1 + \frac{\gamma-1}{2} \frac{u_L}{a_L}\right)^{\frac{2\gamma}{\gamma-1}} \end{pmatrix}, & u_L \leq 0. \end{cases} \quad (25)$$

Here $\varrho_L, u_L, v_L, w_L, p_L$ are prescribed, and $a_L = \sqrt{\gamma p_L / \varrho_L}$. The solution for the first component of the velocity u_B is equal to the prescribed velocity $u_* = 0$ in this special case.

7. Examples

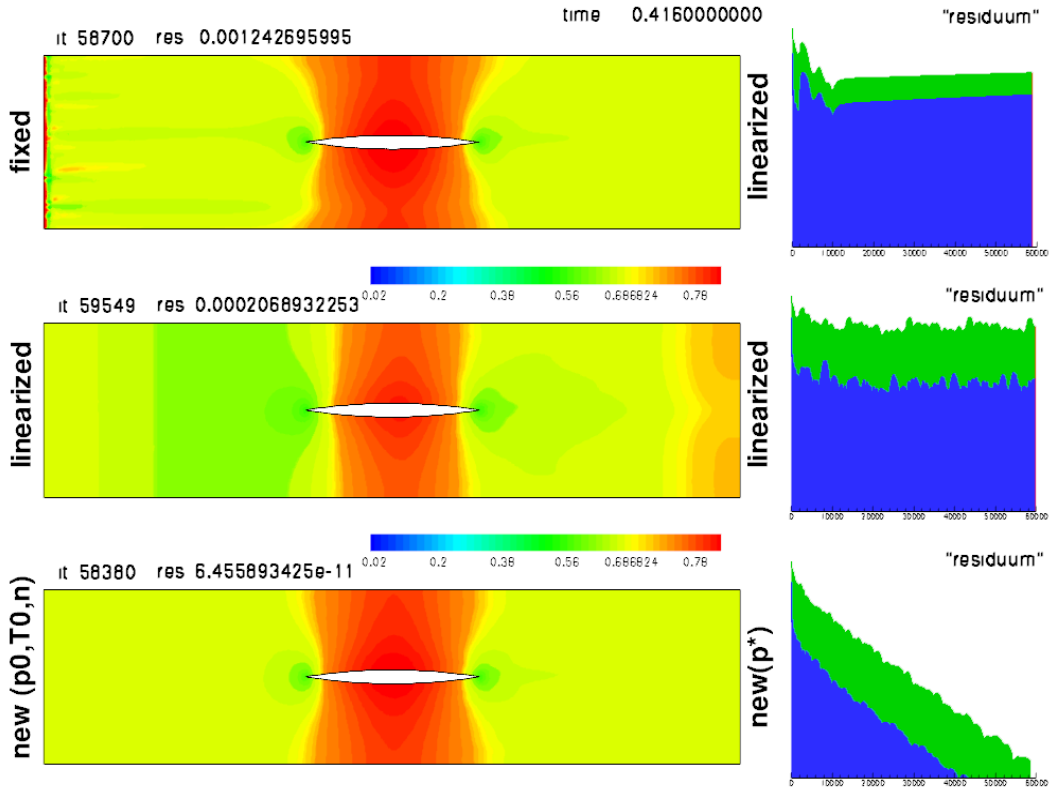


Figure 5: Incompressible flow, body in the channel. Comparison of the various boundary conditions.

Here we present a computational result of the 2D non-stationary inviscid channel flow at Mach number $M = 0.67$. A body immersed in the flowing fluid establishes a certain wave pattern which evolves in time and eventually exits the channel. At Figure 1. we show, that the fixed (values are fixed at the boundary) and linearized (as described in Feistauer (2003)) boundary conditions do not give the expected result in time. The inlet is located left, outlet right, other boundaries are considered as wall. The fixed boundary conditions give incorrect

results near boundaries. The linearized boundary condition reflects the waves into the domain, leading to the oscillations in the solution. The new suggested boundary conditions do not suffer from these drawbacks. The residual behavior (shown right) demonstrates this result.

8. Conclusions

In this paper we worked with the system of equations describing the compressible fluid flow in 2D and 3D. We applied the finite volume method for the discretization of these equations. In order to discretize the values at the boundary we solved the modification of the local Riemann problem. The right-hand side initial-value for this problem was replaced by suitable conditions. On the contrary to the solution of the initial-value Riemann problem, the solution of some modified boundary problems can be written in a closed form. Therefore it is not computationally expensive to use the constructed boundary conditions in the code. The algorithms for the solution of the boundary problems were coded and implemented into own-developed software for the solution of the compressible (laminar or turbulent) gas flow (the Euler equations, the Navier-Stokes equations, the Reynolds-Averaged Navier-Stokes equations) in 2D and 3D. The presented numerical example shows superior behaviour of these boundary conditions.

Acknowledgment

This result originated with the support of Ministry of Industry and Trade of Czech Republic for the long-term strategic development of the research organisation. The authors acknowledge this support.

References

- E. F. Toro 1997: *Riemann Solvers and Numerical Methods for Fluid Dynamics*. Springer, Berlin.
- M. Feistauer 1993: *Mathematical Methods in Fluid Dynamics*. Longman Scientific & Technical, Harlow.
- M. Feistauer, J. Felcman, and I. Straškraba 2003: *Mathematical and Computational Methods for Compressible Flow*. Oxford University Press, Oxford.
- J. Pelant. 1996-2000: Arti reports VZLÚ, z-65, z-67 to z-73. Prague, 1996-2000.
- V. Dolejší 2006: Discontinuous Galerkin method for the numerical simulation of unsteady compressible flow. *WSEAS Transactions on Systems*,5(5):1083-1090.
- M. Kyncl 2011: Numerical solution of the three-dimensional compressible flow. Doctoral Thesis, Charles University, Prague.
- C. J. Kok. 2000: Resolving the dependence on free-stream values for $k - \omega$ turbulence model. *AIAA Journal*, Vol. 38., No. 7..
- David C. Wilcox. 1998: *Turbulence Modeling for CFD*. KNI,Inc.,Anaheim, California, USA.
- M. Kyncl J.Pelant 2012: *Implicit method for the 3D RANS equations with the $k - \omega$ (Kok) turbulent model*. Technical report R5453, VZLÚ, Beranových 130, Prague